Electronic Supplementary Information:[1] Active learning of reactive Bayesian force fields: Application to heterogeneous catalysis dynamics of H/Pt

Jonathan Vandermause,*,† Yu Xie,‡ Jin Soo Lim,¶ Cameron J. Owen,¶ and Boris Kozinsky*,‡,§

†*Department of Physics, Harvard University, Cambridge, Massachusetts 02138, USA*

‡*John A. Paulson School of Engineering and Applied Sciences, Harvard University, Cambridge, MA 02138, USA*

¶*Department of Chemistry and Chemical Biology, Harvard University, Cambridge, MA 02138, USA*

§*Robert Bosch LLC, Research and Technology Center, Cambridge, MA 02142, USA*

E-mail: jonathan_vandermause@g.harvard.edu; bkoz@g.harvard.edu

Table of contents

1 Additional data on training & simulation

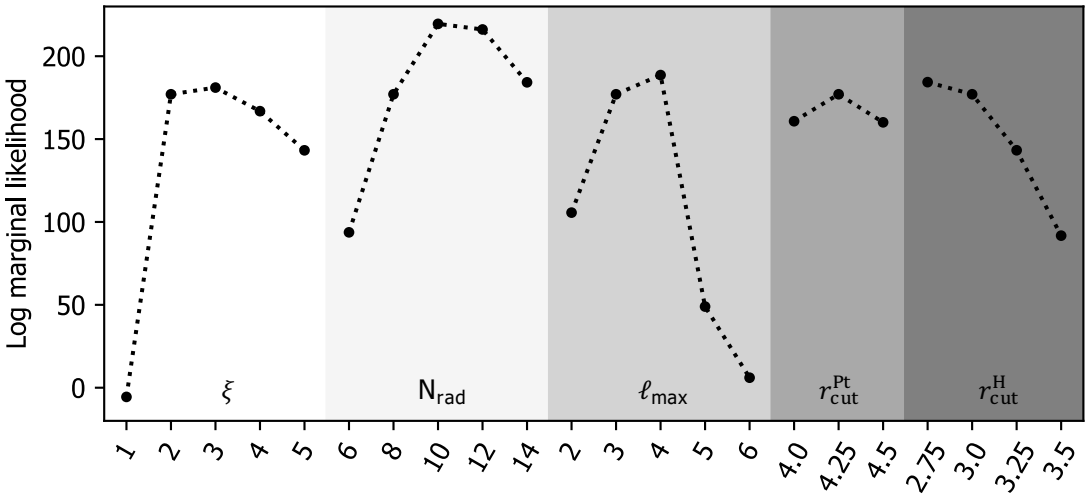

Figure S 1: The SGP likelihood for various integer kernel powers ξ, basis set expansion parameters N_{rad} and ℓ_{max}, and model cutoffs $r_{\mathrm{cut}}^{\mathrm{Pt}}$ (denoting the Pt-Pt cutoff) and $r_{\mathrm{cut}}^{\mathrm{H}}$ (denoting the Pt-H and H-H cutoffs, set equal to each other). The likelihood was evaluated with five structures in the training set of the SGP from the H/Pt(111) training simulation.

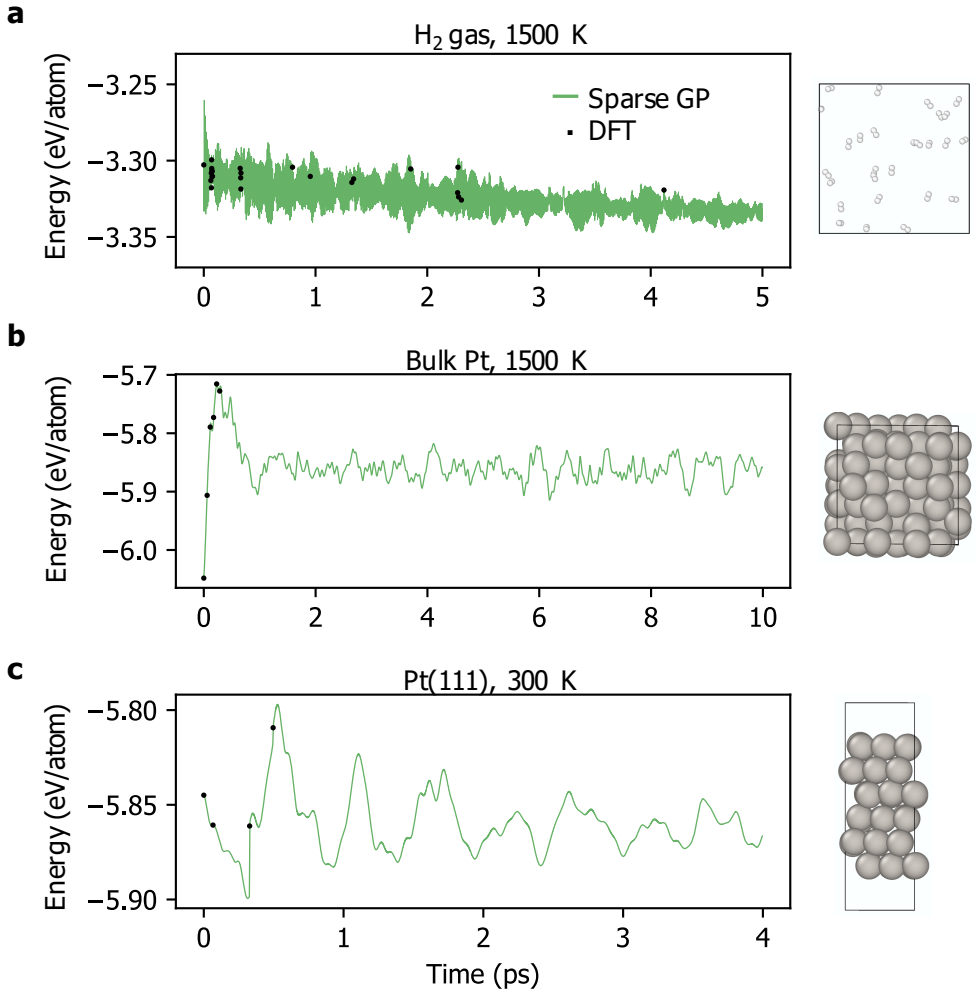

Figure S 2: Potential energy versus time for the on-the-fly training simulations reported in the main text: (a) H_2 gas at 1500 K; (b) bulk Pt at 1500 K; and (c) a six-layer slab model of Pt(111) at 300 K. Example structures from the simulations are shown on the right.

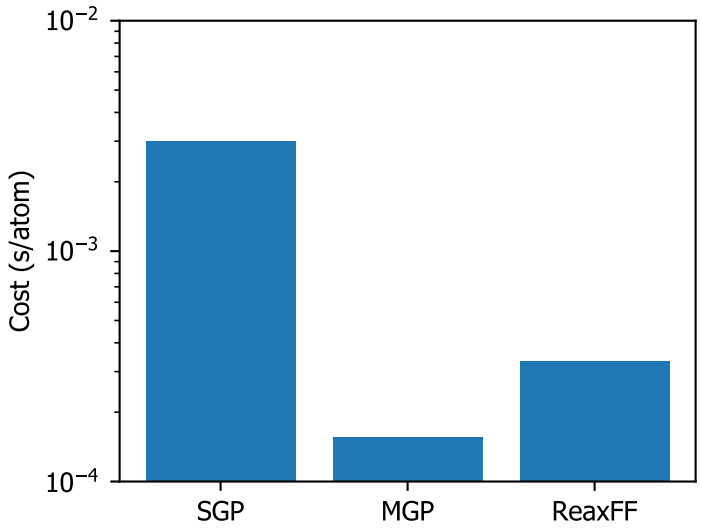

Figure S 3: Prediction cost of the SGP, the equivalent mapped model implemented in LAMMPS (labeled MGP), and the H/Pt ReaxFF model.[2] A single CPU was used to evaluate the models on the same structure, which consisted of a single H atom adsorbed on a six-layer slab model of a 3×3 unit cell of Pt(111).

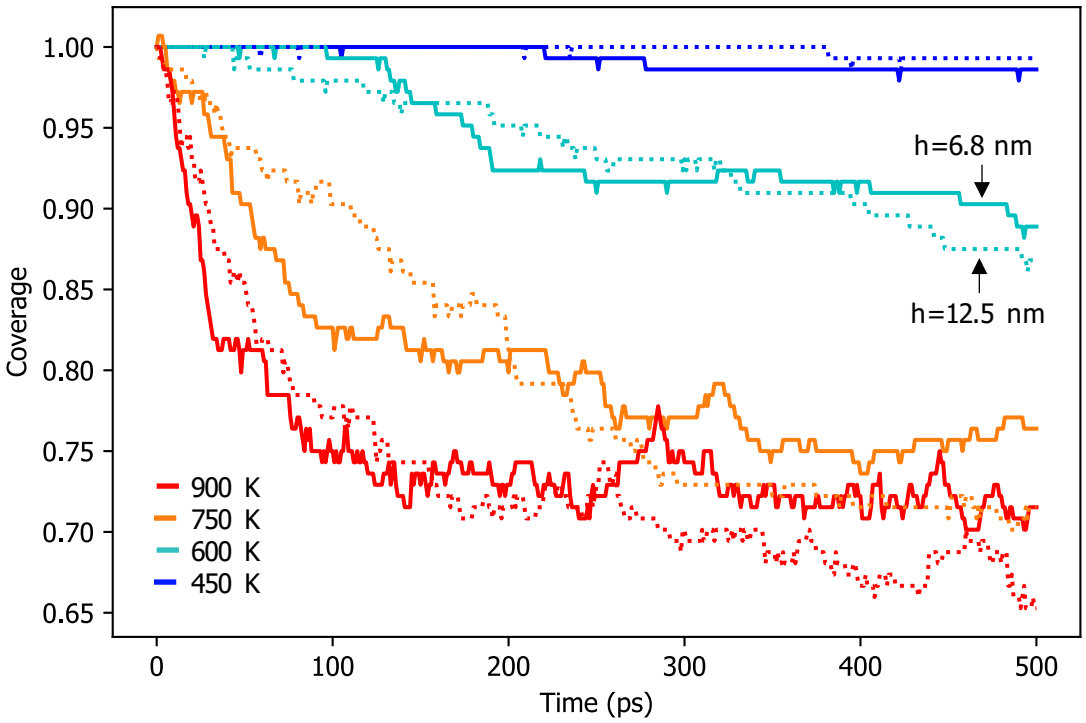

Figure S 4: Surface H coverage versus time for the large-scale MD simulations. Two box heights are considered: 6.8 nm (solid) and 12.5 nm (dotted).

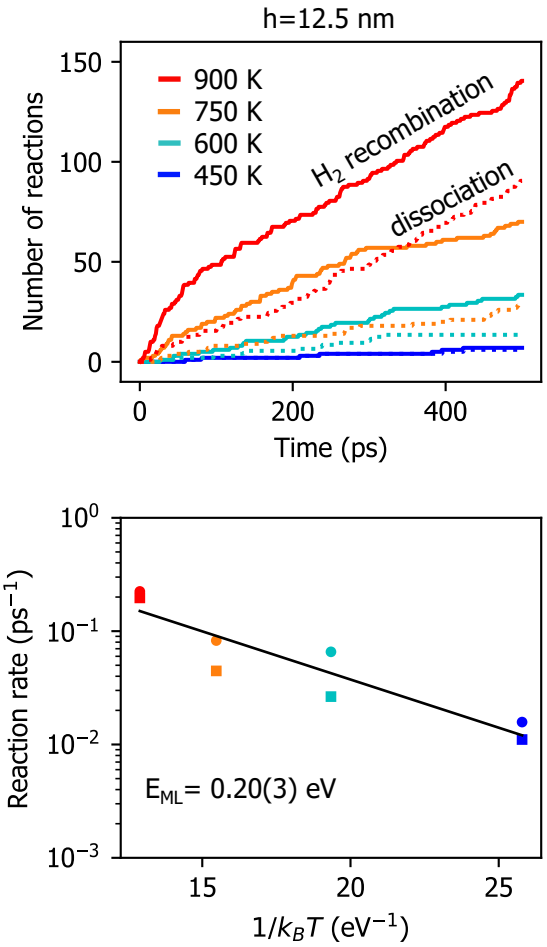

Figure S 5: Cumulative number of H_2 reactive events (top) and the corresponding Arrhenius plot (bottom) for the simulations conducted with the box height of 12.5 nm.

2 Mean absolute errors, parity plots, & comparisons with ReaxFF

Table S1: Mean absolute errors (MAE) of the predictions of the SGP model and the ReaxFF model[2] with respect to DFT for three major properties: (i) atomic force components of Pt and H; (ii) total potential energy; and (iii) virial stress tensor components, including the trace. The predictions are made on 500-ps trajectories generated independently by both models. The MAE values are colored by high (red), medium (orange), and low (green). See Figs. S7-S9 for the corresponding parity plots.

Property	Force field	Component	SGP trajectory	ReaxFF trajectory
Forces (meV/Å)	SGP	Pt	91	133
		H	74	257
	ReaxFF	Pt	631	512
		H	676	598
Energy (meV/atom)	SGP	Total	1.7	26
	ReaxFF	Total	33	93
Virial stress (meV/Å^3)	SGP	Tr	0.6	2.2
		xx	0.8	1.4
		yy	0.7	1.4
		zz	1.4	3.9
		xy	0.4	0.3
		yz	0.6	0.6
		xz	0.6	0.6
	ReaxFF	Tr	15.7	11.2
		xx	31.9	16.1
		yy	31.8	16.6
		zz	16.5	2.4
		xy	1.7	1.4
		yz	2.2	1.8
		xz	2.5	1.1

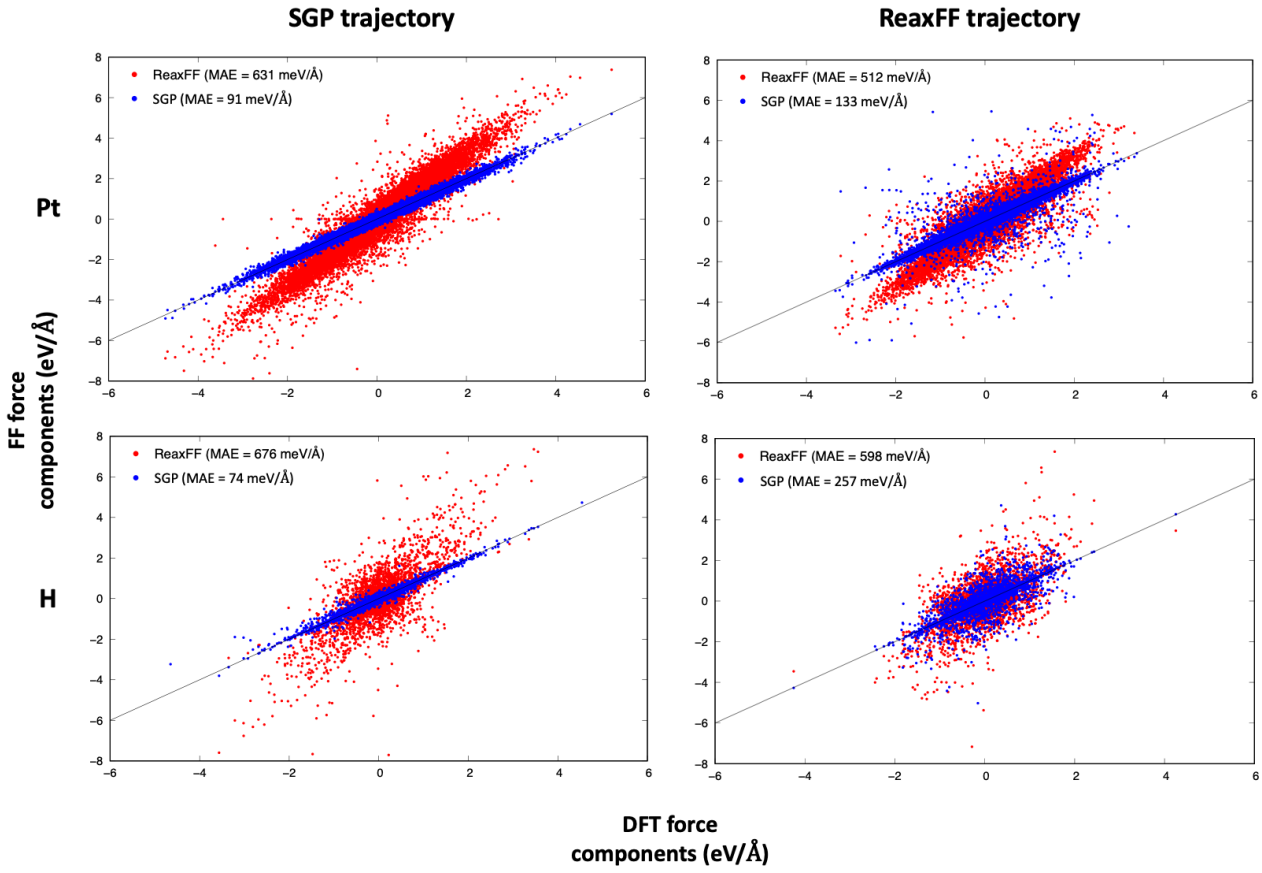

Figure S 6: Parity plot of the force components predicted by the force field (FF) vs. DFT for Pt and H (top and bottom), evaluated on the SGP and ReaxFF trajectories (left and right). The parity lines are shown in black. Predictions of the SGP model and the ReaxFF model[2] are shown in blue and red, respectively. The mean absolute error (MAE) values are indicated in the legend (see Table S1).

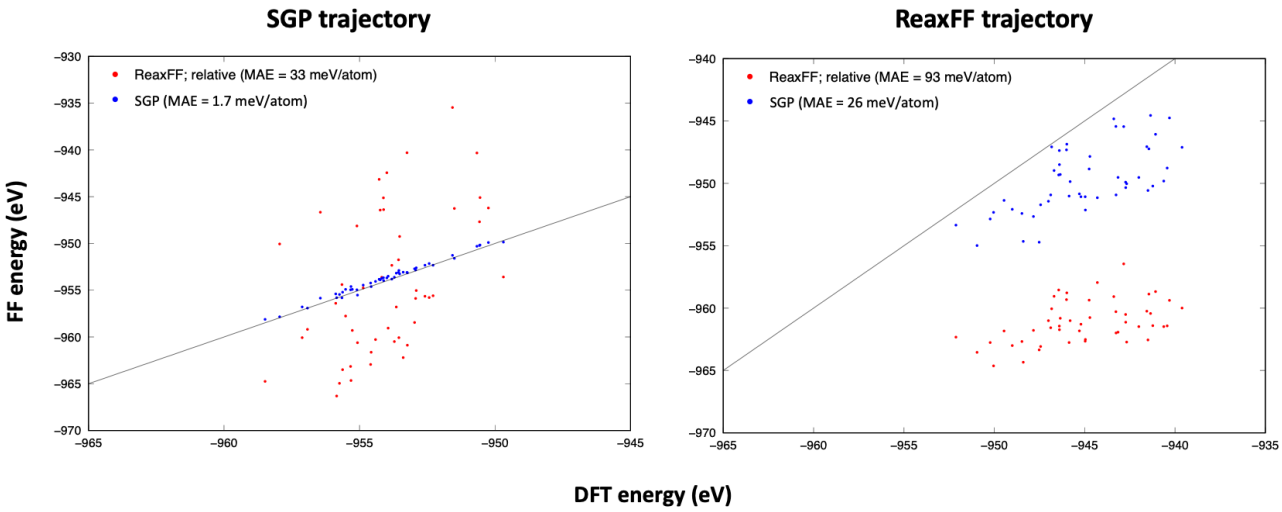

Figure S 7: Parity plot of the potential energies predicted by the force field (FF) vs. DFT, evaluated on the SGP and ReaxFF trajectories (left and right). The parity lines are shown in black. Predictions of the SGP model and the ReaxFF model[2] are shown in blue and red, respectively. The mean absolute error (MAE) values are indicated in the legend (see Table S1, main text). To align the reference, the ReaxFF energy values were shifted by the DFT energy value of the initial relaxed structure.

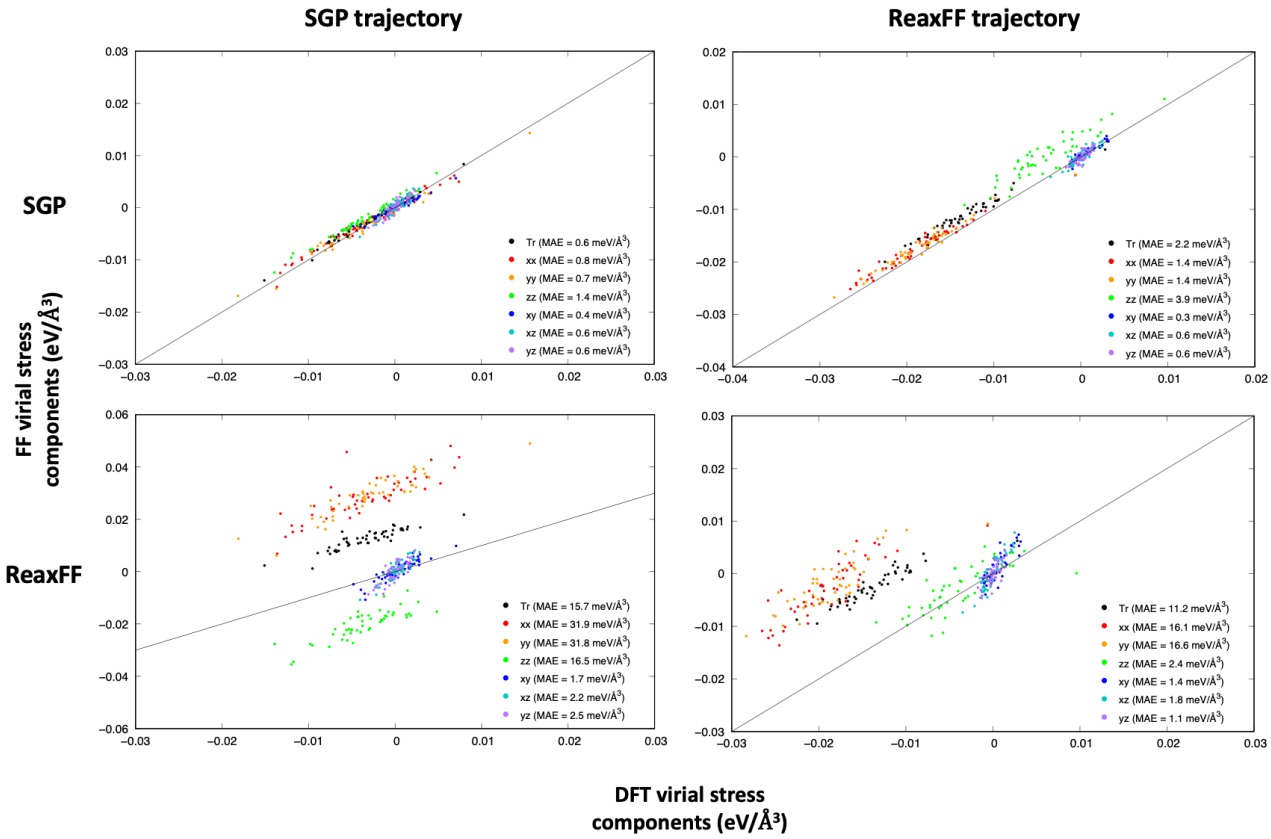

Figure S 8: Parity plot of the virial stress components predicted by the force field (FF) vs. DFT, evaluated on the SGP and ReaxFF trajectories (left and right). The parity lines are shown in black. Predictions of the SGP model and the ReaxFF model[2] are shown in top and bottom, respectively. The six components and the trace are labeled by different colors, with the corresponding mean absolute error (MAE) values indicated in the legend (see Table S1, main text).

3 Transition state pathways

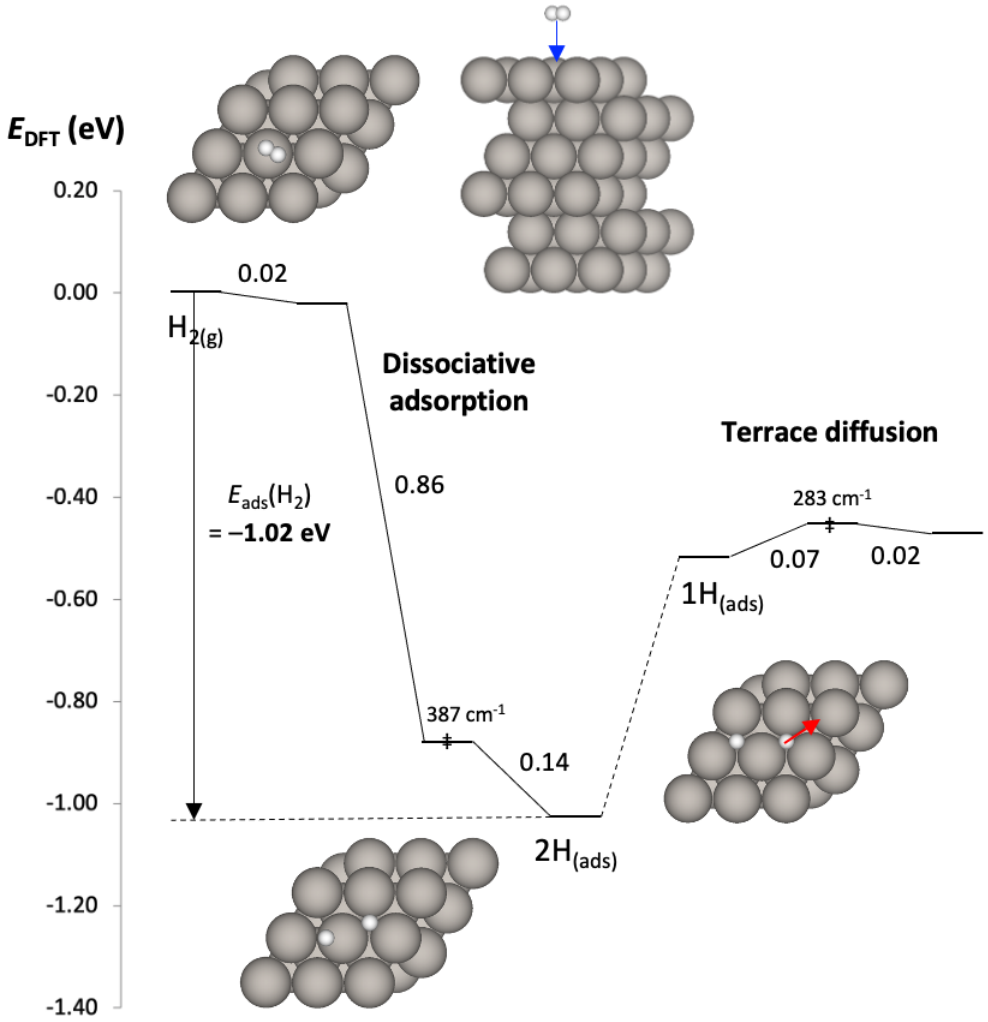

Figure S 9: Minimum energy pathway for H_2 dissociative adsorption and atomic H diffusion on Pt(111), optimized using DFT. Numbers indicate energy differences between adjacent states. Transition states are labeled with ‡, above which the corresponding imaginary frequency is shown. The dotted line indicates a change of reference from $H_{2(g)}$ to $\frac{1}{2}H_{2(g)}$ for $1H_{(ads)}$ states.

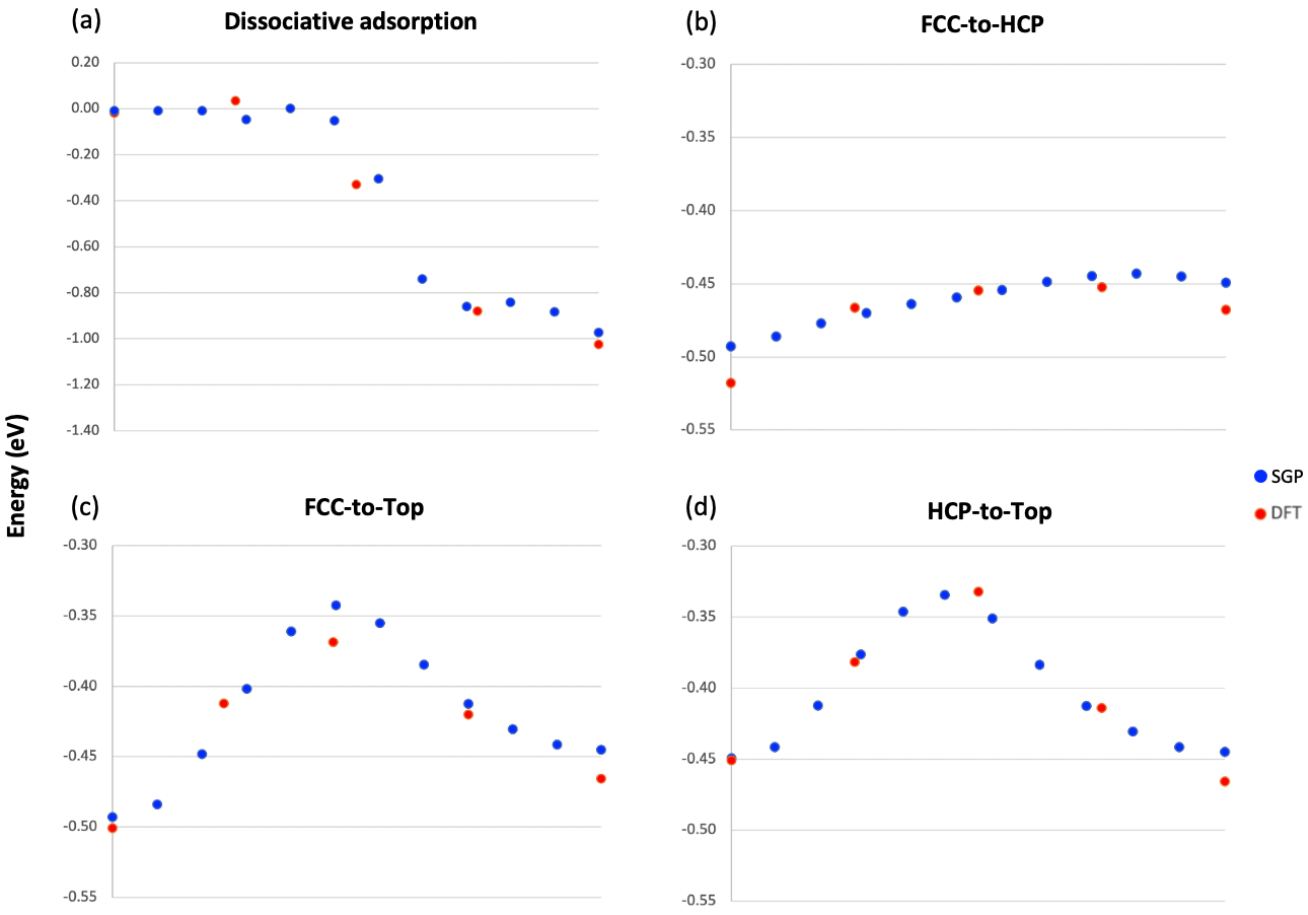

Figure S 10: Transition state pathways for (a) H_2 dissociative adsorption; and atomic H diffusion on Pt(111): (b) FCC to HCP hollow; (c) FCC hollow to atop; (d) HCP hollow to atop. In all cases, our SGP model (blue) is in good agreement with DFT (red). The references for the chemisorption and diffusion processes are $H_{2(g)}$ and $\frac{1}{2}H_{2(g)}$, respectively.

4 Arrhenius analysis of atomic H diffusion

We simulate atomic H diffusion on Pt(111) with our SGP model at 300-900 K for 200 ps (see Sec. C.3, Methods). For the starting structure, we use a 10×10 unit cell of Pt(111) with one H atom placed at the FCC hollow site. As shown in Fig. S11, linear surface diffusion is maintained up to ∼900 K, above which nontrivial vertical motion of the H atom is observed, either desorption or subsurface diffusion, as seen in e.g. large fluctuation of the z-component of the MSD at 1200 K.

The diffusion coefficient is defined as

$$D = \lim_{t\to\infty} \frac{\langle [r(t) - r(0)]^2 \rangle}{2dt}, \tag{S1}$$

where r is the adatom position, time zero is set to the beginning of the linear diffusive regime, and $d = 3$ is the dimensionality of the system. The MSD is ensemble-averaged over 30 independent simulations to ensure sufficient noise reduction. Temperature dependence of the diffusion coefficient shows an Arrhenius behavior (Fig. S12),

$$\ln(D) = \ln(D_0) - \frac{E_\mathrm{a}}{k_\mathrm{B}T}, \tag{S2}$$

from which the corresponding activation energy (E_a) and diffusion prefactor (D_0) are obtained as 92 meV and 3.53×10^{13} Å^2/s, respectively. As the temperature range of 300-900 K corresponds to an average thermal energy of $k_\mathrm{B}\,T$ = 26-78 meV, which lies below the obtained barrier of 92 meV, the simulated diffusion remains a thermally activated process.

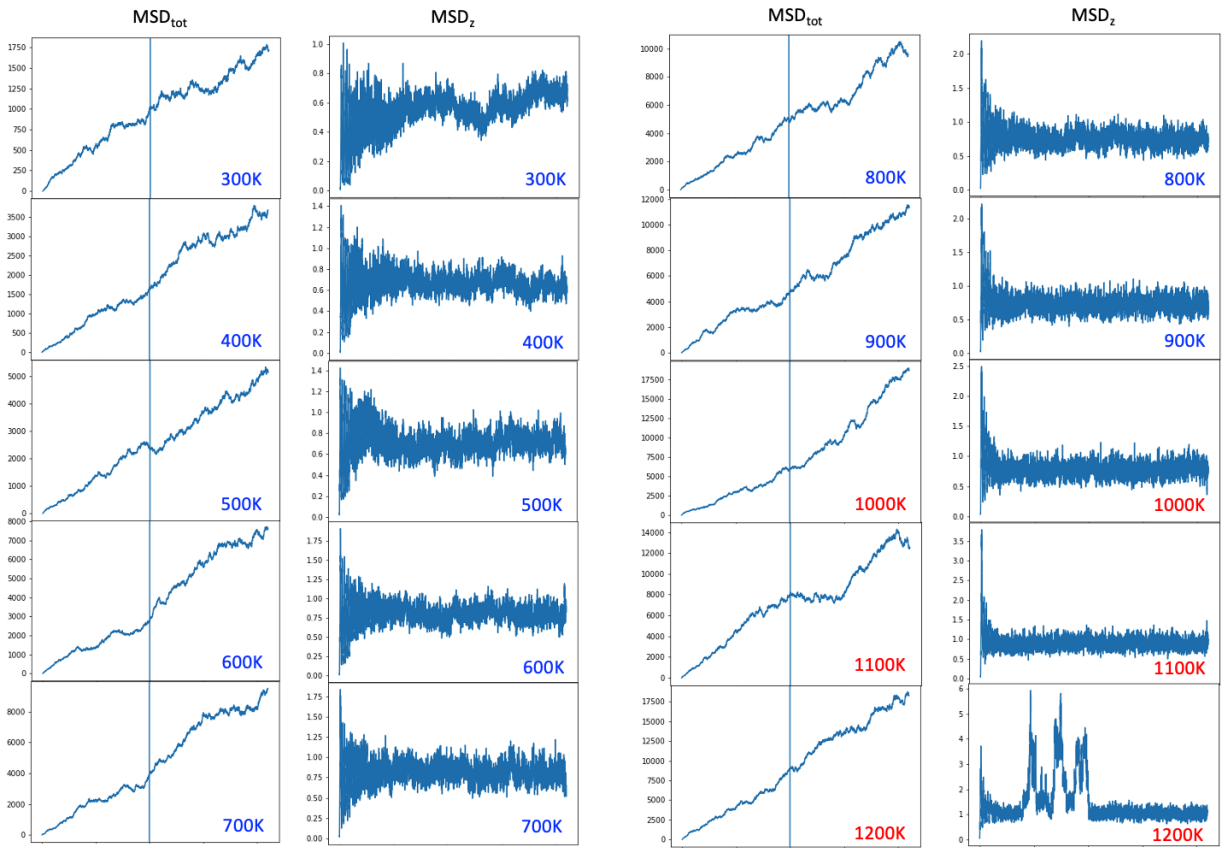

Figure S 11: Plots of ensemble-averaged mean-squared displacement (MSD) (Å^2) of H atom on Pt(111) over 200 ps at 300-1200 K, showing the total MSD (MSD$_{\text{tot}}$) and the corresponding z-component (MSD$_z$). The second half of the simulations (half-time indicated by vertical lines) are taken as linear diffusive regimes. Above 900 K, nontrivial vertical motion of the H atom is detected.

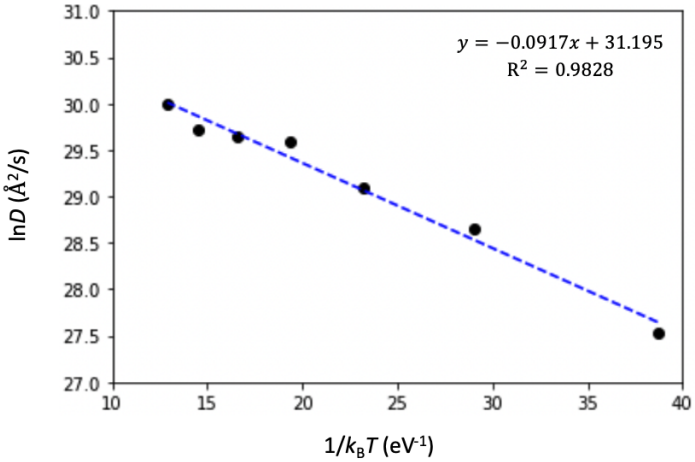

Figure S 12: Arrhenius plot of simulated atomic H diffusion on Pt(111) at 300-900 K.

5 H_2 reactivity simulations with ReaxFF

Using the exact same starting structure—a six-layer slab model of a 12×12 unit cell of Pt(111) with 1 ML H coverage on both sides of the slab and 80 randomly oriented H_2 molecules in the gas phase—we also simulate H_2 reactivity using the ReaxFF model[2] at the same temperature range of 300-900 K. As shown in Fig. S13, ReaxFF leads to facile surface evaporation of isolated Pt hydride units at 600 K and above, ultimately resulting in surface vacancy clusters. As such, the Arrhenius analysis was not performed for this model.

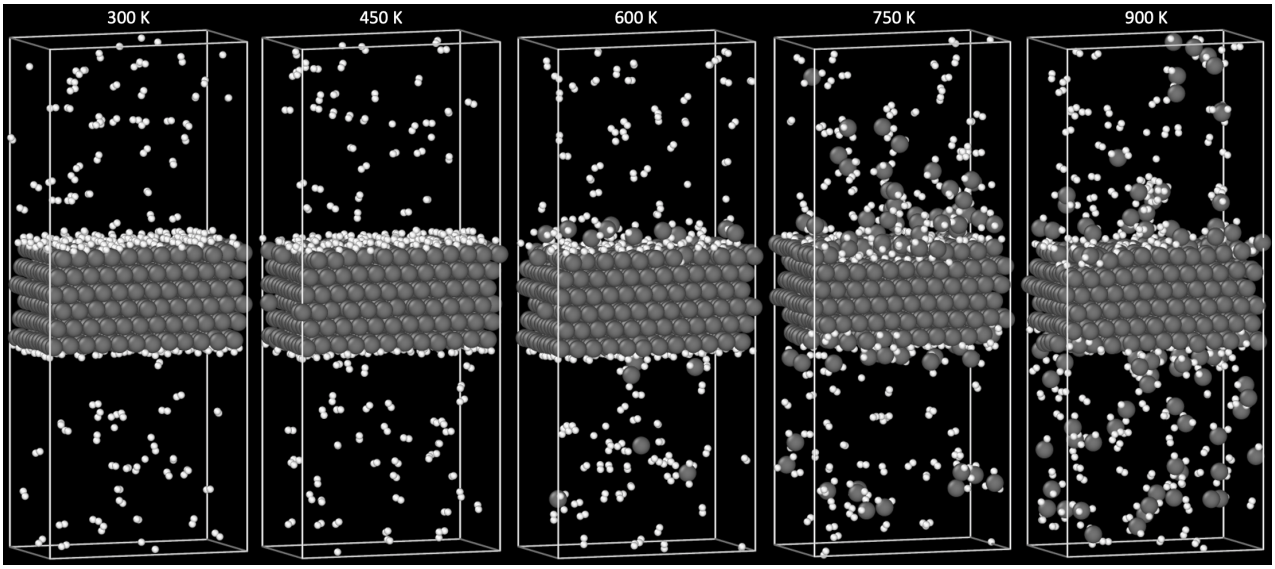

Figure S13: Final snapshots of 500 ps simulations of H_2 reactivity on Pt(111) at 300-900 K, using the ReaxFF model.[2] At 600 K and above, the surface undergoes facile evaporation of gaseous Pt hydride (see Sec. 2 for validation against DFT).

References

(1) We use the abbreviations defined in the main text.

(2) Gai, L.; Shin, Y. K.; Raju, M.; van Duin, A. C. T.; Raman, S. Atomistic Adsorption of Oxygen and Hydrogen on Platinum Catalysts by Hybrid Grand Canonical Monte Carlo/Reactive Molecular Dynamics. *JOURNAL OF PHYSICAL CHEMISTRY C* **2016**, *120*, 9780–9793, DOI: 10.1021/acs.jpcc.6b01064.